Acta Crystallographica Section F
Structural Biology and Crystallization Communications
ISSN 1744-3091

Structure of the His269Arg mutant of the rat aldose reductase-like protein AKR1B14 complexed with NADPH

Krithika Sundaram,[a] Satoshi Endo,[b] Toshiyuki Matsunaga,[b] Nobutada Tanaka,[c] Akira Hara[b] and Ossama El-Kabbani[a]*

[a]Medicinal Chemistry and Drug Action, Monash Institute of Pharmaceutical Sciences, Monash University, 381 Royal Parade, Parkville, Victoria 3052, Australia, [b]Laboratory of Biochemistry, Gifu Pharmaceutical University, Daigaku-Nishi, Gifu 501-1196, Japan, and [c]School of Pharmaceutical Sciences, Showa University, Shinagawa-ku, Tokyo 142-8555, Japan

Correspondence e-mail: ossama.el-kabbani@monash.edu

Received 24 February 2012
Accepted 27 February 2012

PDB Reference: His269Arg AKR1B14, 3qkz.

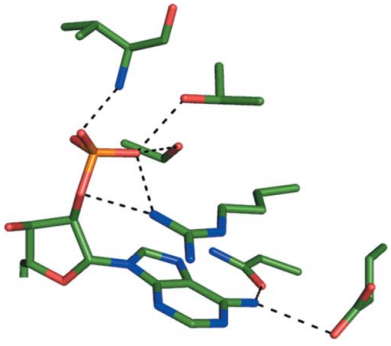

Rat aldose reductase-like protein (AKR1B14) is an orthologue of mouse vas deferens protein (AKR1B7) and plays roles in the detoxification of reactive aldehydes and synthesis of prostaglandin $F_{2\alpha}$. Here, the 1.87 Å resolution crystal structure of the His269Arg mutant of AKR1B14 complexed with NADPH is described and shows that the negatively charged 2′-phosphate group of the coenzyme forms an ionic interaction with the positively charged guanidinium group of Arg269 that is also observed in the human aldose reductase (AKR1B1) structure. Previous experiments on the site-directed mutagenesis of His269 to Arg, Phe and Met revealed fourfold, sevenfold and 127-fold increases in the K_m for NADPH, respectively, which are in agreement with the present molecular-modelling and X-ray crystallographic studies. This is the first tertiary structure of a mutant form of this AKR1B7 orthologue to be reported in order to investigate the structure–function relationship of the nonconserved His269 and its role in coenzyme binding.

1. Introduction

The aldo–keto reductases (AKRs) are an emerging superfamily of monomeric NAD(P)(H)-dependent oxidoreductases that are found in all organisms. They act on a wide range of substrates such as aldehydes, steroids, prostaglandins, monosaccharides, aromatic hydrocarbons *etc.* (Jin & Penning, 2007; Mindnich & Penning, 2009). In mammals, these AKRs also play a central role in the metabolism of a vast range of substrates, drugs, carcinogens and reactive aldehydes, leading to either their bioactivation or detoxication. Thus, mammalian AKRs are considered to be important drug targets (Barski *et al.*, 2008).

All members of the AKR superfamily exhibit a conserved TIM-barrel protein fold consisting of eight α-helices and eight parallel β-strands surrounded by three large loops and include an NADP(H)-binding motif (Jez *et al.*, 1997). The active-site pocket is present at the C-terminal end of the β-sheet. The hydrophobic nature of this pocket favours aromatic and apolar substrates over highly polar substrates. The amino-acid residues that form the $(\alpha/\beta)_8$-barrel are fairly conserved and are believed to play a role in maintaining the overall structure of the protein, in contrast to the residues belonging to the loop regions, which display the greatest variation in amino-acid sequence and determine substrate specificity (Jez & Penning, 2001).

Aldose reductases (ARs) belong to the AKR1B subfamily, in which human AR is named AKR1B1. AR catalyzes the first step in the polyol pathway that is implicated in the development of secondary diabetic complications (Yabe-Nishimura, 1998; Dunlop, 2000; Oates, 2008). It is also involved in the metabolism of retinoids, steroids and xenobiotics, and defensive mechanisms against oxidative stress (Wermuth & Monder, 1983; Crosas *et al.*, 2003; Petrash, 2004; Conklin *et al.*, 2007). Recent studies have identified several rodent AR-like proteins which exhibit high overall amino-acid sequence identity (67–71%) to AR (Srivastava *et al.*, 1998; Lefrançois-Martinez *et al.*, 1999; Val *et al.*, 2002; Endo, Matsunaga, Kuragano *et al.*, 2010; Salabei *et al.*, 2011).

In rats, AKR1B14 has highest amino-acid sequence identity (87%) to the corresponding mouse AR-like protein AKR1B7 (Val *et al.*, 2002). Both AKR1B14 and AKR1B7 show prostaglandin $F_{2\alpha}$ synthase activity (Lambert-Langlais *et al.*, 2009) and also display broad substrate specificity for various aldehydes, α-dicarbonyl compounds and some aromatic ketones (Lefrançois-Martinez *et al.*, 1999; Martinez *et al.*, 2001; Endo, Matsunaga, Fujita *et al.*, 2010). However, the two enzymes differ in their K_m value for the coenzyme NADP(H). The value for AKR1B14 is lower than that for AKR1B7, which is similar to that for AKR1B1 (Kubiseski & Flynn, 1995; Endo, Matsunaga, Fujita *et al.*, 2010; Endo *et al.*, 2011).

The crystal structure of the NADPH binary complex of AKR1B14 has recently been determined and showed unique electrostatic and π-stacking interactions between the NADPH molecule and His269 of the enzyme (Sundaram *et al.*, 2011). His269 is not conserved in other rodent AR-like proteins and ARs including AKR1B1. Site-directed mutagenesis of His269 to Arg, Phe and Met decreased the affinity for the coenzyme (Sundaram *et al.*, 2011), suggesting a pivotal role of His269 in the coenzyme binding. In this study, we report the high-resolution crystal structure of the His269Arg mutant AKR1B14 complexed with NADPH and validate the reported kinetic binding constants of the coenzyme for the His269Phe and His269Met mutants (Sundaram *et al.*, 2011) using molecular modelling.

2. Materials and methods

2.1. Preparation of His269Arg mutant AKR1B14

The pCold IV expression plasmid (Takara) harbouring the cDNA for the His269Arg mutant enzyme was prepared as described previously (Sundaram *et al.*, 2011). The mutant enzyme was expressed in *Escherichia coli* BL21 (DE3) pLysS cells transformed with the expression plasmid and purified to homogeneity as described previously (Chung *et al.*, 2009).

2.2. Crystallization

Crystals of the AKR1B14 His269Arg binary complex were grown using the hanging-drop vapour-diffusion method in a crystallization buffer consisting of 0.1 *M* HEPES pH 7.5, 20% polyethylene glycol 4000 and 5% 2-propanol (optimization of Hampton Research Crystal Screen condition No. 41) at 295 K as described previously (Sundaram *et al.*, 2011). Briefly, the protein and NADPH were mixed in a 1:3 molar ratio and the final concentration of the protein in the binary complex was 22.6 mg ml^{-1}. Droplets consisting of 2 µl of the binary complex solution mixed with an equal volume of crystallization buffer were placed on siliconized cover slips and equilibrated at 295 K against 1 ml crystallization buffer placed in the well. Within one week, crystals were observed with a maximum dimension of approximately 0.2 mm. The crystals were found to be isomorphous to the crystals of wild-type AKR1B14. Crystals selected for X-ray diffraction analysis were soaked in a cryoprotectant solution consisting of 20% glycerol in the crystallization buffer and then flash-cooled at 100 K.

2.3. X-ray data collection and structural determination

X-ray diffraction data were collected at 100 K on a MAR 345 image plate mounted on a Rigaku RU-300 rotating-anode generator (operating at 50 kV and 90 mA). The exposure time (10 min), oscillation range (1°) and crystal-to-detector distance (150 mm) were adjusted to optimize data collection and obtain well resolved spots. X-ray diffraction data were collected from a single crystal which diffracted to 1.87 Å resolution and the data were processed using *HKL*-2000 and *SCALEPACK* (Otwinowski & Minor, 1997). Auto-indexing of the data confirmed that the mutant enzyme crystallized in the monoclinic space group $P2_1$, with unit-cell parameters a = 50.85, b = 69.30, c = 87.95 Å, β = 96.0°. The Matthews coefficient (V_M) was calculated to be 2.13 Å^3 Da^{-1}, with an estimated solvent content of 42% (Matthews, 1968).

Table 1
Data-collection and refinement statistics.

Values in parentheses are for the highest resolution shell.

Data collection and processing	
Space group	$P2_1$
Unit-cell parameters (Å, °)	a = 50.85, b = 69.30, c = 87.95, β = 96.0
Radiation source	Rotating anode
Wavelength (Å)	1.54178
Diffraction data	
Resolution (Å)	30–1.87 (1.91–1.87)
No. of unique reflections (possible)	48259 (4159)
No. of unique reflections (measured)	46136 (3581)
Multiplicity	3.4 (2.8)
Completeness (%)	95.6 (86.1)
$\langle I/\sigma(I)\rangle$	20.8 (5.4)
R_{merge} (%)	3.7 (11.6)
Refinement statistics	
Resolution (Å)	30–1.87
Protein residues	630
Solvent molecules	668
NADPH molecules	2
R_{free}† (%)	23.2
R_{cryst} (%)	16.4
R.m.s.d.s	
Bonds (Å)	0.021
Angles (°)	1.7
Ramachandran plot, residues in (%)	
Most favoured regions (%)	92
Allowed regions (%)	8
Luzzati mean coordinate error (Å)	0.21
Mean B factors (Å^2)	
Protein	17.4
NADPH	16.2

† The same reflections were used as for the wild type.

The crystal structure of the AKR1B14 His269Arg mutant in complex with NADPH was determined by molecular replacement using *MOLREP* from the *CCP*4 suite of crystallographic programs (Winn *et al.*, 2011). The atomic coordinates of wild-type AKR1B14 (PDB code 3o3r; Sundaram *et al.*, 2011) were used as the search model, excluding the coenzyme and solvent molecules. The rotation and translation functions of *MOLREP* identified two molecules per asymmetric unit. The initial model was subjected to rigid-body refinement, which produced a well defined $F_o - F_c$ difference electron-density map for the coenzyme. The two NADPH molecules were fitted into the electron density using *Coot* and the structure was refined using *REFMAC*5 (Murshudov *et al.*, 2011; Emsley & Cowtan, 2004). This was followed by iterative cycles of manual fitting of amino-acid side chains and solvent molecules into $2F_o - F_c$ and $F_o - F_c$ difference electron-density maps and the structure after refinement was validated using *PROCHECK* (Laskowski *et al.*, 1993). The final model was a crystallographic dimer comprising a total of 630 amino-acid residues, two NADPH molecules and 668 solvent molecules.

2.4. Molecular modelling of the AKR1B14 His269Phe and His269Met mutants

His269 in AKR1B14 was mutated to Phe and Met using *Coot* and the structures were processed and energy-minimized using the Protein Preparation and Prime modules in the *Maestro* software

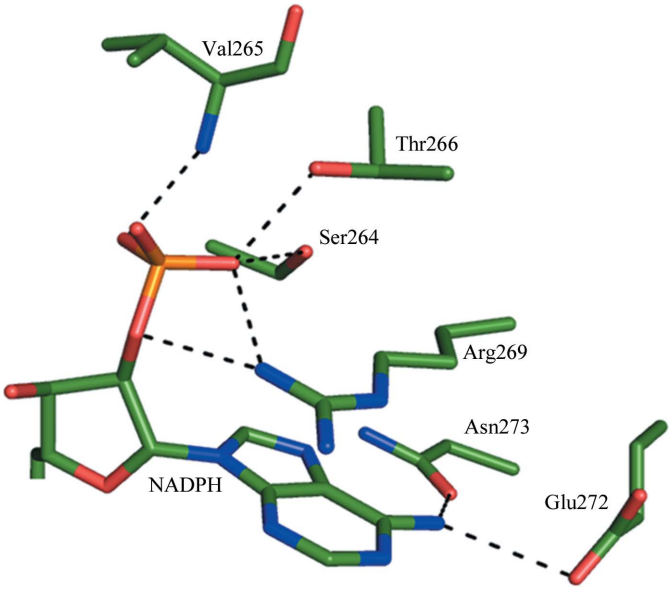

Figure 1
Interactions between the AKR1B14 His269Arg mutant and coenzyme in the vicinity of the adenosine 2′-phosphate moiety of NADPH. Hydrogen bonds and ionic interactions are represented by black broken lines.

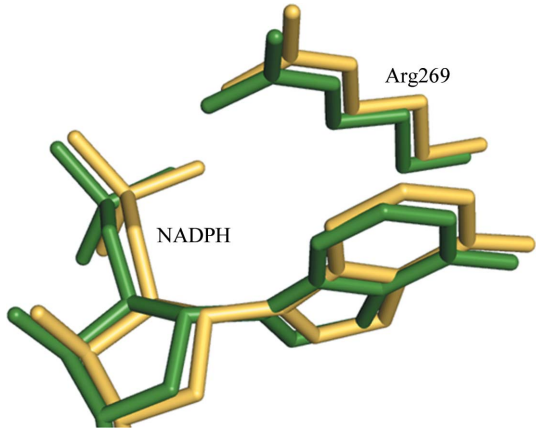

Figure 2
Superimposition of the crystal structures of the AKR1B14 His269Arg mutant (green) and AKR1B1 (gold) in the vicinity of the adenosine 2′-phosphate moiety of NADPH, showing the corresponding Arg269 side chains. The r.m.s.d. of non-H atoms was 0.52 Å.

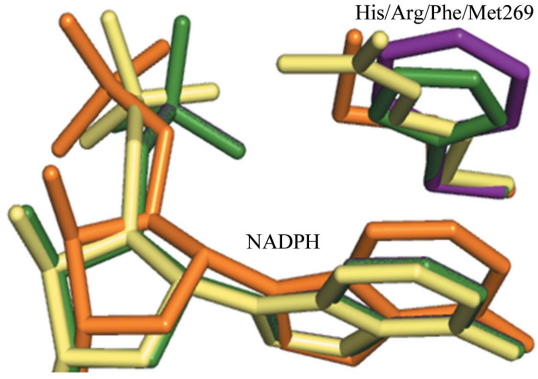

Figure 3
Superimposition of the models of wild-type (green), His269Arg (yellow), His269Phe (purple) and His269Met (orange) AKR1B14 in the vicinity of the adenosine 2′-phosphate moiety of NADPH. For clarity, only the corresponding side chains at position 269 are shown.

package v.8.5 (Schrödinger LLC) as described previously (Zhao *et al.*, 2010). The final outputs were saved and the figures were generated using *PyMOL* (http://www.pymol.org).

3. Results and discussion

The crystal structure of the AKR1B14 His269Arg mutant in complex with NADPH was refined at 1.87 Å resolution with a final R_{cryst} of 16.4% and R_{free} of 23.2%. The backbone dihedral angles of 92% of the residues were in the favoured regions and the remaining 8% were in the allowed regions of the Ramachandran plot. A summary of the data-collection and refinement statistics is presented in Table 1. The residues that participated in interactions with the NADPH molecule were found to be identical to those observed in the AKR1B14 wild-type structure (Sundaram *et al.*, 2011), with the exception of the side chain of the mutated Arg269, which formed ionic interactions with the 2′-phosphate group (Fig. 1) in addition to the stacking interaction of its guanidinium group with the adenine ring of the NADPH (Sundaram *et al.*, 2011). Upon superimposition of the crystal structures of the AKR1B14 His269Arg mutant and AKR1B1 (PDB entry 1pwl; El-Kabbani *et al.*, 2004) complexed with NADPH, it was revealed that the orientations of the Arg residues and adenosine 2′-phosphate moieties of NADPH were similar (Fig. 2).

In an earlier study, site-directed mutagenesis of His269 in AKR1B14 to Arg showed a more than fourfold increase in the K_m value for NADPH compared with that of the wild-type enzyme (Sundaram *et al.*, 2011). The present crystal structure confirmed that the decrease in affinity on mutation arises from alteration of the interaction between the adenine ring of NADPH and the imidazole ring of His269 observed in the structure of the wild-type enzyme. Since the His269Phe and His269Met mutations resulted in larger impairments in NADP(H) binding (Sundaram *et al.*, 2011), we performed molecular-modelling studies of the two mutant enzymes. In the model of His269Phe mutant AKR1B14 the phenyl ring of the mutated Phe269 was found to be oriented in a similar manner to the His269 imidazole ring of the AKR1B14 wild-type structure (Fig. 3), forming a π-stacking interaction with the adenine ring of the NADPH. However, the side chain of Phe269 lacked the additional hydrogen-bond interaction observed in the wild-type AKR1B14 between the 2′-phosphate group of NADPH and the ND1 of the imidazole ring of His269 (Sundaram *et al.*, 2011), which contributes to the sevenfold increase in the K_m value for NADPH. The energy-minimized structure of the AKR1B14 His269Met mutant (Fig. 3) illustrated that the largest loss in affinity for NADP(H) arising from the mutation resulted from the loss of both hydrogen-bonding and π-stacking interactions between His269 of the wild-type AKR1B14 and the coenzyme. Interestingly, the replacement of His269 in the wild-type enzyme by the non-aromatic residues Arg or Met resulted in a shift in the 2′-phosphate group of the coenzyme, while the orientations of the coenzyme in the wild-type and His269Phe structures were virtually superimposable (Fig. 3).

4. Conclusion

Crystallographic and modelling studies of the binding of coenzyme to AKR1B14 confirmed that the π-stacking interaction between the imidazole ring of the nonconserved His269 and the adenine ring of the coenzyme and the hydrogen bond between ND1 of His269 and the 2′-phosphate group of the coenzyme are both important for binding of the coenzyme. While the replacement of His269 by Arg resulted in a fourfold increase in the K_m value for NADPH, the loss

of the hydrogen-bond interaction in the His269Phe mutant and both π-stacking and hydrogen-bond interactions in the His269Met mutant were responsible for the sevenfold and 127-fold increases in the K_m value, respectively (Sundaram *et al.*, 2011).

References

Barski, O. A., Tipparaju, S. M. & Bhatnagar, A. (2008). *Drug Metab. Rev.* **40**, 553–624.

Chung, R., Endo, S., Hara, A. & El-Kabbani, O. (2009). *Acta Cryst.* F**65**, 395–397.

Conklin, D., Prough, R. & Bhatanagar, A. (2007). *Mol. Biosyst.* **3**, 136–150.

Crosas, B., Hyndman, D. J., Gallego, O., Martras, S., Parés, X., Flynn, T. G. & Farrés, J. (2003). *Biochem. J.* **373**, 973–979.

Dunlop, M. (2000). *Kidney Int. Suppl.* **77**, S3–12.

El-Kabbani, O., Darmanin, C., Schneider, T. R., Hazemann, I., Ruiz, F., Oka, M., Joachimiak, A., Schulze-Briese, C., Tomizaki, T., Mitschler, A. & Podjarny, A. (2004). *Proteins*, **55**, 805–813.

Emsley, P. & Cowtan, K. (2004). *Acta Cryst.* D**60**, 2126–2132.

Endo, S., Matsunaga, T., Fujita, A., Kuragano, T., Soda, M., Sundaram, J., Dhagat, U., Tajima, K., El-Kabbani, O. & Hara, A. (2011). *Biochimie*, **93**,1476–1486.

Endo, S., Matsunaga, T., Fujita, A., Tajima, K., El-Kabbani, O. & Hara, A. (2010). *Biol. Pharm. Bull.* **33**, 1886–1890.

Endo, S., Matsunaga, T., Kuragano, T., Ohno, S., Kitade, Y., Tajima, K., El-Kabbani, O. & Hara, A. (2010). *Arch. Biochem. Biophys.* **503**, 230–237.

Jez, J. M., Bennett, M. J., Schlegel, B. P., Lewis, M. & Penning, T. M. (1997). *Biochem. J.* **326**, 625–636.

Jez, J. M. & Penning, T. M. (2001). *Chem. Biol. Interact.* **130–132**, 499–525.

Jin, Y. & Penning, T. M. (2007). *Annu. Rev. Pharmacol. Toxicol.* **47**, 263–292.

Kubiseski, T. J. & Flynn, T. G. (1995). *J. Biol. Chem.* **270**, 16911–16917.

Lambert-Langlais, S., Pointud, J.-C., Lefrançois-Martinez, A.-M., Volat, F., Manin, M., Coudoré, F., Val, P., Sahut-Barnola, I., Ragazzon, B., Louiset, E., Delarue, C., Lefebvre, H., Urade, Y. & Martinez, A. (2009). *PLoS One*, **4**, e7309.

Laskowski, R. A., Moss, D. S. & Thornton, J. M. (1993). *J. Mol. Biol.* **231**, 1049–1067.

Lefrançois-Martinez, A.-M., Tournaire, C., Martinez, A., Berger, M., Daoudal, S., Tritsch, D., Veyssière, G. & Jean, C. (1999). *J. Biol. Chem.* **274**, 32875–32880.

Martinez, A., Aigueperse, C., Val, P., Dussault, M.-H., Tournaire, C., Berger, M., Veyssière, G., Jean, C. & Lefrançois Martinez, A.-M. (2001). *Chem. Biol. Interact.* **130–132**, 903–917.

Matthews, B. W. (1968). *J. Mol. Biol.* **33**, 491–497.

Mindnich, R. D. & Penning, T. M. (2009). *Hum. Genomics*, **3**, 362–370.

Murshudov, G. N., Skubák, P., Lebedev, A. A., Pannu, N. S., Steiner, R. A., Nicholls, R. A., Winn, M. D., Long, F. & Vagin, A. A. (2011). *Acta Cryst.* D**67**, 355–367.

Oates, P. J. (2008). *Curr. Drug Targets*, **9**, 14–36.

Otwinowski, Z. & Minor, W. (1997). *Methods Enzymol.* **276**, 307–326.

Petrash, J. M. (2004). *Cell. Mol. Life Sci.* **61**, 737–749.

Salabei, J. K., Li, X.-P., Petrash, J. M., Bhatnagar, A. & Barski, O. A. (2011). *Chem. Biol. Interact.* **191**, 177–184.

Srivastava, S., Harter, T. M., Chandra, A., Bhatnagar, A., Srivastava, S. K. & Petrash, J. M. (1998). *Biochemistry*, **37**, 12909–12917.

Sundaram, K., Dhagat, U., Endo, S., Chung, R., Matsunaga, T., Hara, A. & El-Kabbani, O. (2011). *Bioorg. Med. Chem. Lett.* **21**, 801–804.

Val, P., Martinez, A., Sahut-Barnola, I., Jean, C., Veyssière, G. & Lefrançois-Martinez, A. M. (2002). *Endocrinology*, **143**, 3435–3448.

Wermuth, B. & Monder, C. (1983). *Eur. J. Biochem.* **131**, 423–426.

Winn, M. D. (2011). *Acta Cryst.* D**67**, 235–242.

Yabe-Nishimura, C. (1998). *Pharmacol. Rev.* **50**, 21–33.

Zhao, H.-T., Soda, M., Endo, S., Hara, A. & El-Kabbani, O. (2010). *Eur. J. Med. Chem.* **45**, 4354–4357.